Super-resolution mapping of gravel bed surface roughness using terrestrial laser scanning and airborne laser scanning

Guo-Hao Huang[a] and Chi-Kuei Wang[b*]

[a] Postdoctoral Fellow, Department of Geomatics, National Cheng-Kung University, No.1, University Road, Tainan City 701, Taiwan; Tel: + 886-6-2757505#63825; E-mail: guohao.huang@gmail.com

[b] Associate Professor , Department of Geomatics, National Cheng-Kung University, No.1, University Road, Tainan City 701, Taiwan; Tel: + 886-6-2757505#63809; E-mail: chikuei@mail.ncku.edu.tw

*Corresponding author: chikuei@mail.ncku.edu.tw

ABSTRACT

The aim of this study is to derive the scaling behavior of gravel-bed roughness of terrestrial laser scanning (TLS) from airborne laser scanning (ALS). We use the fractal dimension, which can be estimated from the slope of log-log variogram of laser scanning data, to represent gravel-bed roughness. The study area is located near the confluence of the Nan-Shih River and Pei-Shih River, northern Taiwan. Two gravel-bed sites with the extent of 6m × 6m were acquired by FARO photon 80, and then in-situ digital surface models (DSMs) were generated with 1 cm × 1cm resolution. ALS survey was conducted by an Optech ALTM 3070 at the density of 247 points/m^2. The point cloud data were collected by ALS, which showed smoothed surface of TLS counterparts. In this study, we used the deconvolution procedure to derive the variograms of TLS-derived DSM from the variograms of ALS data. Hence, we could establish the link between the gravel-bed roughness of TLS-derived DSM and ALS data. The results will lead a better understanding of gravel-bed roughness using ALS data for the large-scale areas.

Keywords: surface roughness, variogram, downscaling, laser scanning

INTRODUCTION

The determination of gravel-bed roughness is crucial for the understanding of affecting flow resistance and sediment transportation. Moreover, it is established that river bed roughness exhibits multi-scale characteristics (Butler et al., 2001). Numerous studies have found that the gravel-beds surface presents either two-scale (e.g., grain and form scales, where the latter refers to the cluster bedforms) or mono-scale behavior under the investigation of fractal analysis (Robert, 1988; Nikora et al., 1998; Butler et al. 2001; Hodge et al., 2009). The fractal dimension calculated from the log-log variogram is employed for measuring gravel-bed roughness in this study.

The calculation of fractal dimension needs detailed elevation information of the gravel-bed surface. Terrestrial laser scanning (TLS) have been employed to acquire that information in the field, and successfully used to derive the gravel-bed roughness (Hodge et al.; Huang and Wang, 2012). The airborne laser scanning (ALS) system shows the potential of acquiring the surface elevation of a large area. However, the footprint of ALS is larger than that of TLS, which led that the gravel-bed surface measurement would be the smoother for the ALS. Therefore, the gravel-bed roughness derived from ALS data would be biased. As a result, we employed the deconvolution procedure to derive the gravel-bed roughness of TLS data from ALS data in this study.

Deriving the characteristics of point data from areal data is called super-resolution or downscaling in remote sensing. Atkinson (2004) had introduced numerous downscaling approaches, such as sub-pixel classification, Hopfield neural network, and deconvolution procedure. We choose the deconvolution procedure because it can be combined with the calculation of gravel-bed roughness. Hence, we employed the deconvolution procedure to deriving the variogram of TLS data (point support) from the variogram of ALS data (areal support) in this study.

While substantial studies have examined the scaling characteristics of the gravel-bed roughness (Robert, 1988; Nikora et al., 1998; Butler et al., 2001; Hodge et al., 2009; Huang and Wang, 2012), to the best of our knowledge, the ALS data have not yet been used to for this task. We demonstrate that the deconvolution procedure is able to obtain the characteristics of grave-bed roughness of TLS-derived DSMs from the ALS data. This research will lead a better understanding of the scaling characteristics of the gravel-bed roughness on the change of measurement scale.

DATA

The exposed gravel surfaces of two gravel-bed sites, denoted as S1 and S2 are shown in Fig. 1, which are located at the gravel bar near the confluence of the Nan-Shih River and Pei-Shih River, northern Taiwan. There was no vegetation cover for these two sites. TLS was conducted with a FARO Photon 80 laser scanner on May 7th, 2009. The nominal measurement accuracy of FARO Photon 80 is 2 mm (Faro Technology Inc., 2008). We employed the multiple scan strategy to reduce the number of data voids that are due to the obstruction lines of sight by large grains. Four laser scans were conducted at the middle of four edges of the 6 m × 6 m sampling area. The mean-based two-stage filter developed by Wang et al. (2011) was u for deriving the digital surface model (DSM) with an area of 6 m × 6 m and a spatial resolution of 1 cm. The DSM coverage, defined as the ratio of the number of valid cells within the TLS-derived DSM, is more than 94% for S1 and S2. Fig. 2(a) and (b) illustrated the color maps of TLS-derived DSMs and white regions indicate empty cells caused by the obstruction of the line of sight by large grains. At these sites, the grain size distributions were obtained using the photo-sieving technique (Graham et al., 2005) with the image samples taken from a 50 cm ×50 cm frame, and the d_{50} is 5.5 cm. More detailed information regarding the *in situ* TLS measurement can be found in Wang et al. (2011).

Fig. 1. The orthophoto shows the two gravel-bed sites: S1 and S2.

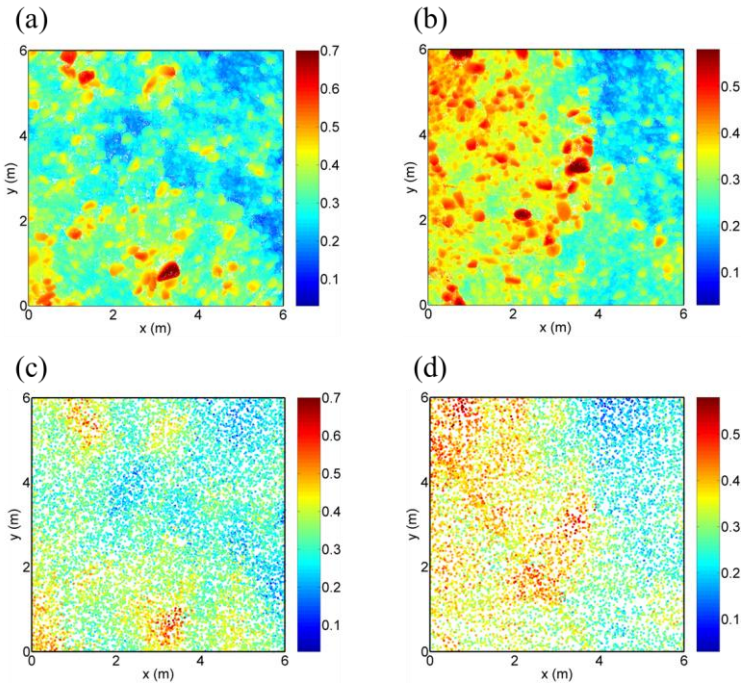

Fig. 2. Color maps of TLS-derived DSM: (a) S1; (b) S2. Color maps of ALS point data: (c) S1; (d) S2 (units: meters).

Airborne laser scanning survey was conducted on May 9th, 2009 at the above ground level (AGL) of 650 m by an Optech ALTM 3070 system with the nominal elevation and horizontal accuracies of 15 and 32.5 cm, respectively (Optech Inc., 2003). The average point cloud density for 2009 datasets is 247 pts/m^2. The color maps of ALS point data for S1 and S2 are shown in Fig. 2(c) and 2(d). The number of points for S1 and S2 is more than 8500 points. Except for manual removal of few extremely high points from the ALS dataset, no other filtering was applied to the point cloud data.

The airborne laser footprint has a diameter of approximately 45 cm on the gravel-bed surface, while the cell of the TLS-derived DSM is 1 cm × 1 cm. As a result, we expected that the gravel-bed surface obtained from ALS data is smoother than that of the TLS-derived DSM.

METHOD

The fractal dimension *D*, calculated from the log-log variogram, can be used to describe the scaling characteristics of the gravel-bed surface (Robert, 1988; Butler et al., 2001). The variogram, which is half the mean squared difference of paired data points separated by the lag vector h, is given by:

$$\hat{\gamma}(\mathbf{h}) = \frac{1}{2N(\mathbf{h})} \sum_{i=1}^{N(\mathbf{h})} [z(\mathbf{x}_i) - z(\mathbf{x}_i + \mathbf{h})]^2 \qquad (1)$$

where $z(\mathbf{x}_i)$ is the elevation at location vector $\mathbf{x}_i$ and $N(\mathbf{h})$ is the number of paired data points separated by the lag vector **h**. In variogram computation, the lag vector **h** is given a lag increment and lag tolerance. The fractal dimension *D* can be estimated from the slope b of the log-log variogram using D = 3 – b/2 (Butler et al., 2001), when the log-log plot of semivariance $\hat{\gamma}(\mathbf{h})$ against lag **h** is linear.

There are usually two fractal bands in the variogram of a gravel surface (Robert, 1988; Butler et al., 2001). The two bands can be viewed as the grain scale and form scale (Robert, 1988), respectively. The form scale can be more easily examined if the stationarity prerequisite is fulfilled, which can be accomplished by removal of the trend surface in data. In this study, the planar trend surface is fitted to the TLS-derived DSMs and ALS data, respectively, and the elevation residuals are used for computing

the variogram.

To connect the variograms of the TLS-derived DSM and ALS point data, which are generated from different supports, a deconvolution procedure is implemented to derive a variogram on the support of TLS-derived DSM from the variogram of ALS point data. For the deconvolution procedure, we used a mathematical model that is conditional negative semidefinite (CNSD) to ensure that the variances of the linear combinations of random variables are non-negative (Webster and Oliver, 2007). And the theoretical variogam model is regularized to fit the variogram of ALS point data iteratively. Since previous studies suggest that gravel-bed roughness presents two distinct scales, the double spherical model is used to represent the two spatial components. In the case of isotropy, the double spherical function can be written as

$$\gamma(h)=\begin{cases} C_o + C_1\left\{\dfrac{3h}{2a_1}-\dfrac{1}{2}\left(\dfrac{h}{a_1}\right)^3\right\}+C_2\left\{\dfrac{3h}{2a_2}-\dfrac{1}{2}\left(\dfrac{h}{a_2}\right)^3\right\} & \text{for } 0 < h \le a_1 \\ C_o + C_1 + C_2\left\{\dfrac{3h}{2a_2}-\dfrac{1}{2}\left(\dfrac{h}{a_2}\right)^3\right\} & \text{for } a_1 < h \le a_2 \\ C_o + C_1 + C_2 & \text{for } h > a_2 \end{cases} \quad (2)$$

swhere the quantity C_0 is the nugget component, a_1 and a_2 are the ranges of the first and second model, respectively, and C_1 and C_2 are the sills of the first and second model, respectively. More detailed information regarding the regularization can be found in Huang and Wang. (2012).

The deconvolution procedure is an iterative procedure. Journel and Huijbregts (1978) proposed this general approach and we modified it as follows.

1. Define a point support model from inspection of the variogram of ALS point data and estimate the parameters (sill, range) using basic deconvolution rules.
2. Compute the theoretically regularized variogram and compare it with the variogram of ALS point data.
3. Adjust the parameters of the point support model so as to bring the regularized model in line with the variogram of ALS point data.

However, Journel and Huijbregts (1978) did not mention how to adjust the parameters of the point support model. In this study, we use genetic algorithm to adjust the parameter, calculate the roughness of the variogram derived from the deconvolution procedure and compare it to the gravel-bed roughness derived from TLS-derived DSMs.

RESULTS AND DISCUSSION

A planar trend surface is fitted to the TLS-derived DSM and ALS data, respectively, and the residual elevations are employed for the compution of variograms to a maximum lag of 300 cm, which is half the size of the 6 m × 6 m TLS-derived DSM. The variograms are calculated for both the TLS-derived DSMs (denoted as dots in Fig. 3) and ALS data (denoted as triangles in Fig. 3). Because the TLS-derived DSMs and ALS data have different number of data points, the lag increments are set to be 1 cm and 15 cm (which are the smallest possible values while avoiding the jagged appearance in the variograms) for the TLS-derived DSMs and ALS data, respectively. The downscaling results are shown in Fig. 3 (denoted as black dashed lines). To enable a direct comparison between downscaling result and variograms of TLS-derived DSMs, offsets are applied to the variograms of TLS-derived DSM for S1 and S2, respectively, to match the sill values of the downscaling result.

As shown in Fig. 3, we found that the downscaling result for S1 and S2 demonstrated grain and form scale in the log-log plot. Moreover, good agreements can be found between the downscaling results (black dashed lines in Fig. 3) and variograms of TLS-derived DSM (dots in Fig. 3) at grain and form scale. We observed that grain scale did not present in the variograms of ALS data, which is consistent with observation of Huang and Wang (2012).

Table 1 listed the gravel-bed roughness estimated from TLS-derived DSMs, ALS data, and downscaling result. Because the footprint of ALS data is larger than the cell of TLS-derived DSM, the gravel-bed roughness(fractal dimension) derived from ALS data would be smaller than that estimated from TLS-derived DSM at form scale. As shown in Fig. 3 and Table 1, we found that the gravel-bed roughness derived from the downscaling results and TLS-derived DSMs are very close. Thus, we obtain the promising results from the deconvolution procedure.

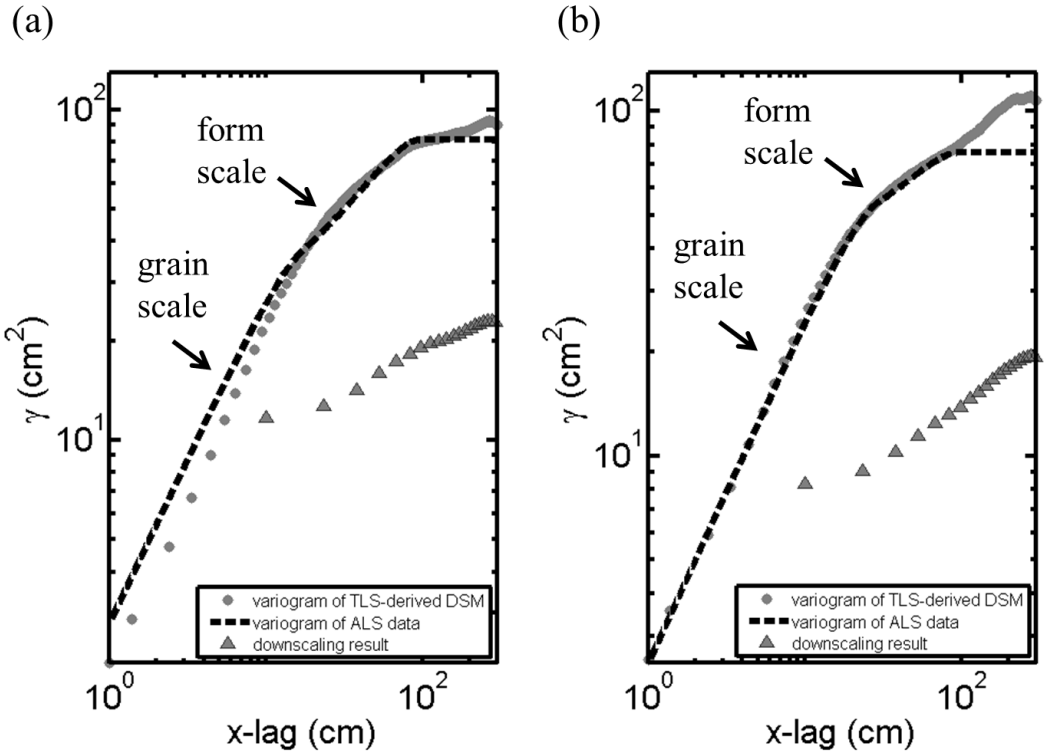

Fig. 3. Comparison between the downscaling result and variogram of TLS-derived DSM: (a) S1; (b) S2.

Table 1. Fractal properties of TLS-derived DSM and ALS Data for S1 and S2

		S1	S2
TLS-derived DSMs	D_1	2.49	2.51
	D_2	2.79	2.85
ALS data	D_1	N/A	N/A
	D_2	2.61	2.54
Downscaling variograms	D_1	2.51	2.51
	D_2	2.78	2.83

* D_1 and D_2 are the fractal dimensions at the grain scale and the form scale, respectively.

CONCLUSIONS

We have demonstrated that the support size plays an important role on interpreting the scaling characteristics of the gravel-bed surface in ALS data. The deconvolution procedure provides an effective way to estimate the scaling behavior of TLS-derived DSMs from ALS data.

The downscaling results establish the link between the scaling behavior of the TLS-derived DSM

and ALS data at grain and form scale. This shows the potential of using the deconvolution procedure to characterize the gravel-bed roughness on the change of measurement scale.

REFERENCES

A. G. Journel and C. J. Huijbregts, "Mining geostatistics," Academic Press, London, 1978.

A. Robert, "Statistical properties of sediment bed profiles in alluvial channels," *Math. Geol.*, vol. 20, pp. 205-225, Apr. 1988.

C.-K. Wang, F.-C. Wu, G.-H. Huang, and C. Y. Lee, "Mesoscale terrestrial laser scanning of fluvial gravel surface," *IEEE Geosci. Remote Sens. Lett.*, vol. 8, pp. 1075-1079, Nov. 2011.

D. J. Graham, I. Reid, and S. P. Rice, "Automated sizing of sediments: coarse-grained Image-processing procedures," *Math. Geol.*, vol. 37, pp. 1-28, Jan. 2005.

Faro Technology Inc., "Faro Photon 80/20 Specification," http://www.faro.com/pdf/FARO_Photon_en.pdf, 2008.

G.-H. Huang and C.-K. Wang, "Multiscale geostatistical estimation of gravel-bed roughness from terrestrial and airborne laser scanning", *IEEE Geoscience and Remote Sensing Letters*, vol. 9, pp. 1084-1088, doi: 10.1109/LGRS.2012.2189351, Nov. 2012.

Goovaerts, P., "Kriging and semivariogram deconvolution in the presence of irregular geographical units, " *Mathematical Geosciences*, vol. 40, pp. 101-128, 2008.

J. B. Butler, S. N. Lane, and J. H. Chandler, "Characterization of the structure of river-bed gravels using two-dimensional fractal analysis," *Math. Geol.*, vol. 33, pp. 301-330, Apr. 2001.

Optech Incorporated, "ALTM 3070 Datasheet", http://www.optech.ca/pdf/Specs/specs_altm_3070.pdf, 2003.

P. M. Atkinson, (2004) Resolution manipulation and sub-pixel mapping (chapter 4). In, de Jong, S. and van der Meer, F. (eds.) *Remote Sensing Image Analysis: Including the Spatial Domain.* Amsterdam, Netherlands, Kluwer Press, pp. 51-70, 2004.

R. Hodge, J. Brasington, and K. Richards, "Analysing laser-scanned digital terrain models of gravel bed surfaces: linking morphology to sediment transport processes and hydraulics," *Sedimentology*, vol. 56, 2024-2043, May 2009.

R. Webster and M. A. Oliver, "Geostatistics for environmental scientists," 2nd ed., John Wiley & Sons, Chichester, 2007.

V. I. Nikora, D. G. Goring, and B. J. F. Biggs, "On gravel-bed roughness characterization," *Water Resour. Res.*, vol. 34, pp. 517-527, Mar. 1998.